Lecture 12

Stellar atmospheres
prof. Marcos Diaz

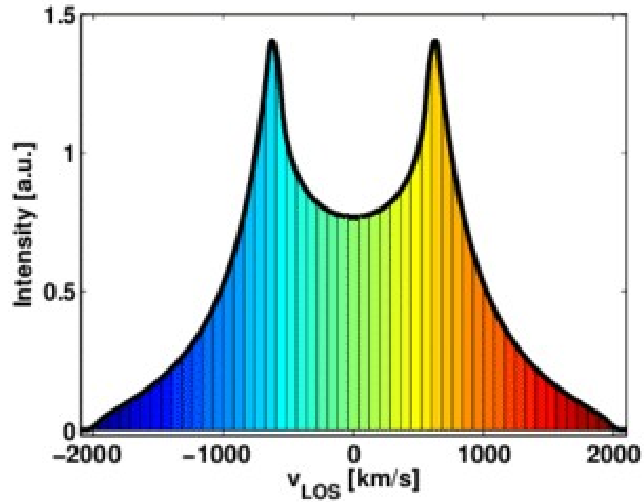

(a)

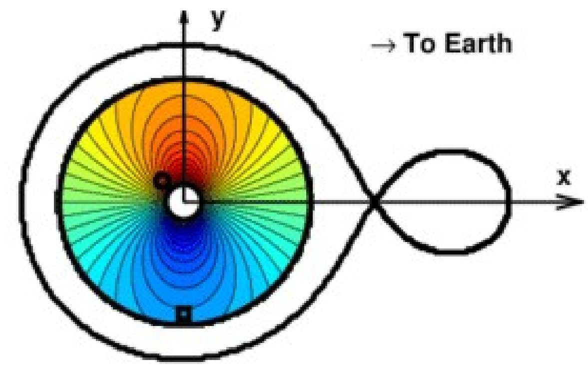

(b)

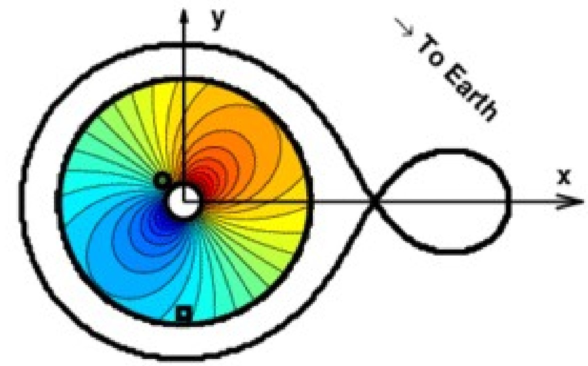

(c)

(from Salewski 2015)

treasure map:

Gray: 254, 423, 458
H&M: pg 617
Bohn-Vitense: pg 124, 125
Rutten: pg 125,123

Microscopic Line Broadening

V. Microturbulence

The macroscopic to thermal energy cascade

$$\Delta l_k \lesssim l_\nu$$

Δl_k = isokinetic coherent scale, l_ν = mean free path

with a symmetric ($\xi^2 = \xi^2_x + \xi^2_y + \xi^2_z$) gaussian vel. field:

$$N(v)\,dv = \frac{1}{\pi^{1/2}\xi} e^{-(v/\xi)^2} dv$$

$$\Delta\lambda_D = \frac{\lambda_0}{c}\left(\frac{2kT}{m} + \xi^2\right)^{1/2} \quad \text{or} \quad \Delta\nu_D = \frac{\nu_0}{c}\left(\frac{2kT}{m} + \xi^2\right)^{1/2}$$

→ *most important line transfer effect: unsaturate lines and increase EW*

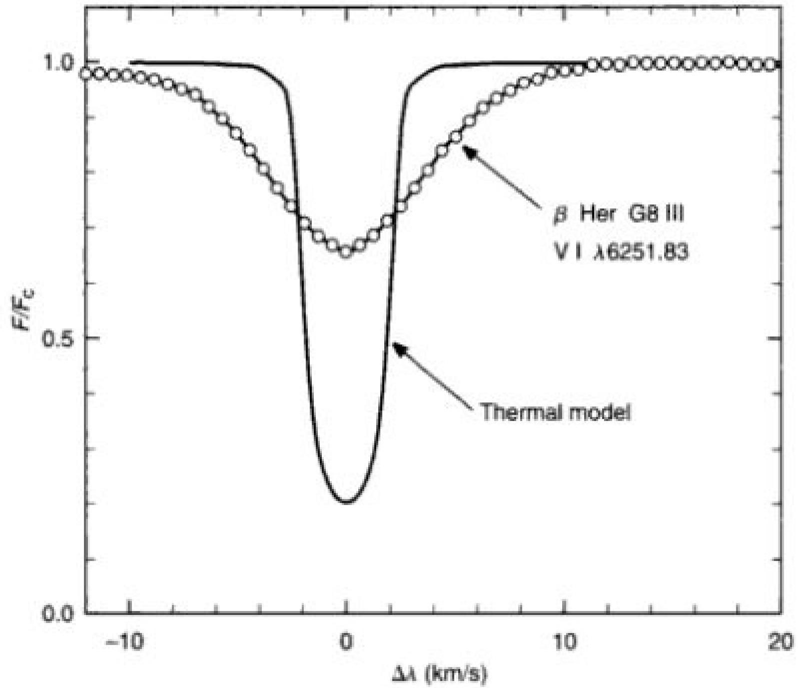

Fig. 17.1. The thermal profile computed from a model photosphere with only thermal broadening does not look much like the real star. Data from the Elginfield Observatory, University of Western Ontario.

from Gray 2005

FWHM(ξ)

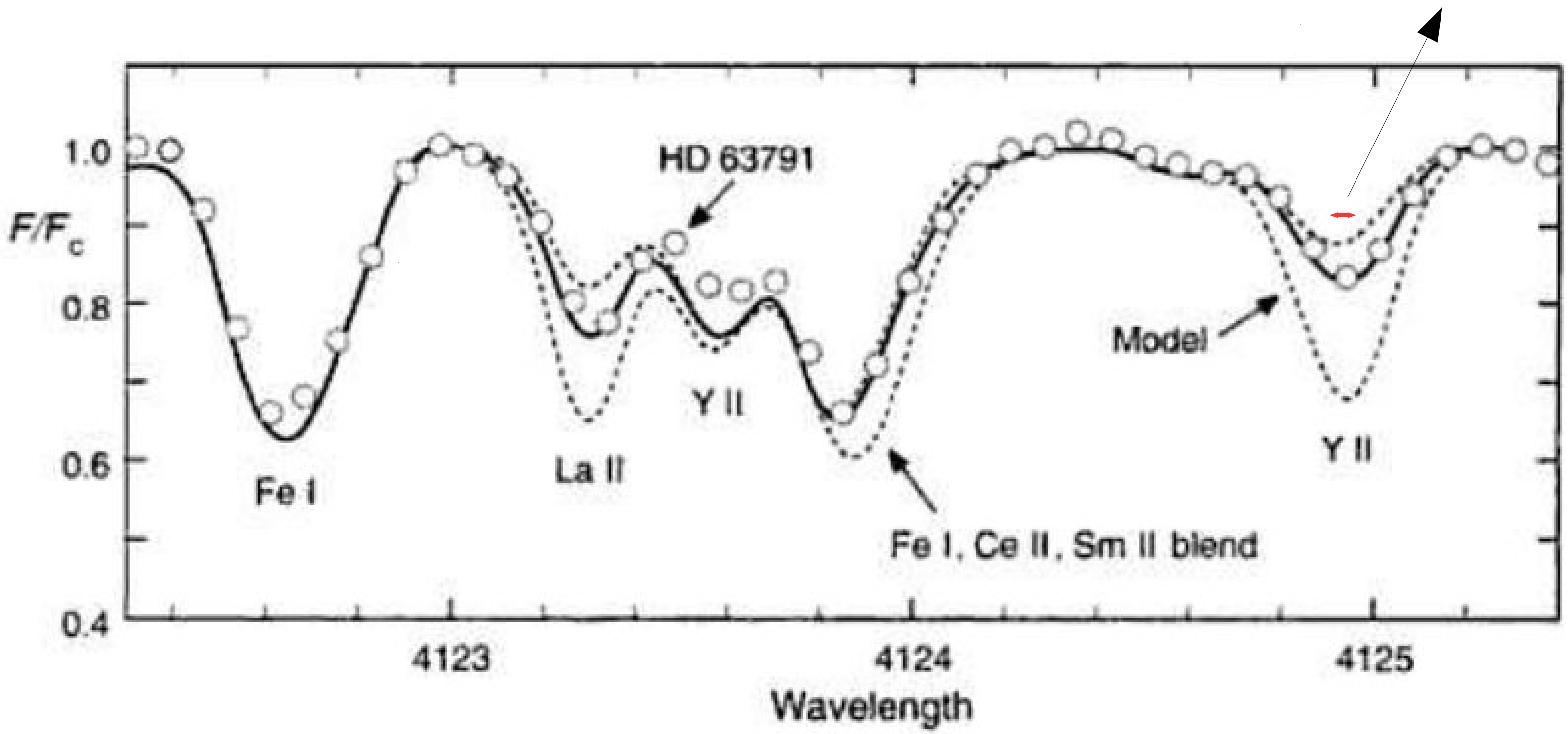

Fig. 16.9. The circles show the observed spectrum, while the lines are for models ($T_{eff} = 4725$ K, $\log g = 1.70$, and $\xi = 1.60$ km/s) with different chemical abundances. The solid line is deemed to fit best. Based on data in Fig. 2 of Burris *et al.* (2000). The resolving power is ~20 000 and the signal-to-noise ratio ~100.

(from Gray 2005)

Macroscopic Line Broadening

I. Stellar rotation

the rotation kernel for spherical stars

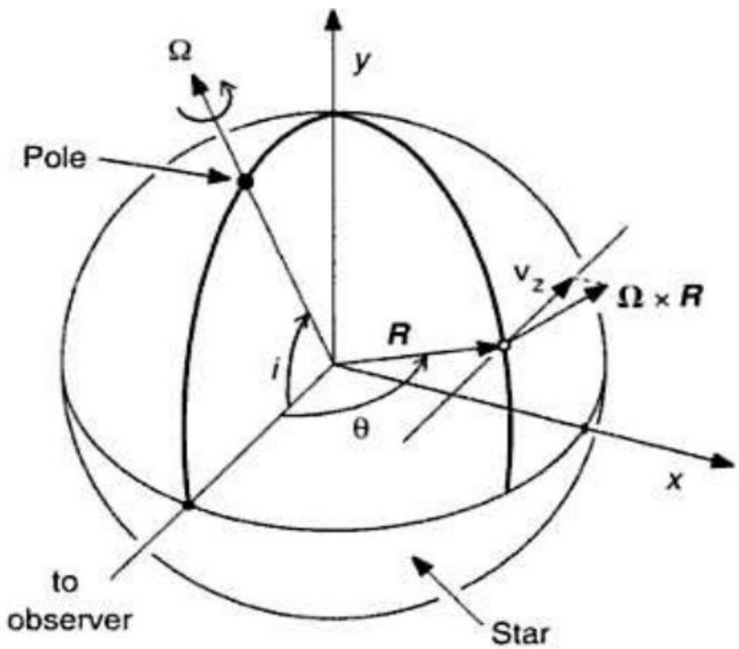

$$\vec{v} = \vec{\Omega} \times \vec{R}_*$$

$$\Omega_x = 0$$

$$\Omega_y = \Omega \sin(i)$$

$$\Omega_z = \Omega \cos(i)$$

$$v_{rad} = -v_z = -x\Omega \sin(i)$$

$$\frac{v_{rad}}{c} = \frac{x\Omega \sin(i)}{c} = \frac{\Delta\lambda}{\lambda} \qquad (1)$$

$$\frac{R_* \Omega \sin(i)}{c} = \frac{\Delta\lambda_L}{\lambda} \qquad x = \frac{\Delta\lambda}{\lambda} \frac{c}{\Omega \sin(i)} = \frac{\Delta\lambda}{\Delta\lambda_L} R_*$$

(Intensity integral over stellar surface)

non-rotating case:

$$\frac{F_\lambda}{F_c} = \frac{\int H(\lambda)\, I_c \cos(\theta)\, d\omega_*}{\int I_c \cos(\theta)\, d\omega_*}$$

$$H_\lambda = I_\lambda \,/\, I_{cont}$$

rotating case:

$$\frac{F_\lambda}{F_c} = \frac{\int H(\lambda - \Delta\lambda)\, I_c \cos(\theta)\, d\omega_*}{\int I_c \cos(\theta)\, d\omega_*}$$

with $(\lambda - \Delta\lambda_{Dopp}) = \lambda_{obs}$

(Intensity integral over stellar surface)

non-rotating case:

$$\frac{F_\lambda}{F_c} = \frac{\int H(\lambda) I_c \cos(\theta) d\omega_*}{\int I_c \cos(\theta) d\omega_*}$$

$$H_\lambda = I_\lambda / I_{cont}$$

rotating case:

$$\frac{F_\lambda}{F_c} = \frac{\int H(\lambda-\Delta\lambda) I_c \cos(\theta) d\omega_*}{\int I_c \cos(\theta) d\omega_*}$$

with $(\lambda - \Delta\lambda_{Dopp}) = \lambda_{obs}$

$$dx = \frac{d(\Delta\lambda)}{\Delta\lambda_L} R_*$$

$$d\omega_* = \frac{dA}{R_*^2} = \frac{dxdy}{\cos(\theta) R_*^2}$$

$$F_\lambda = \int_{-R_*}^{R_*} \int_{y_1}^{y_2} H(\lambda-\Delta\lambda) \frac{I_c}{R_*^2} dxdy$$

$I_c(\theta)$ = constant - no limb darkening

$$F_\lambda = \frac{I_c}{R_*^2}\int_{-R_*}^{R_*}\int_{-y_1}^{y_1} H(\lambda-\Delta\lambda)\,dx\,dy$$

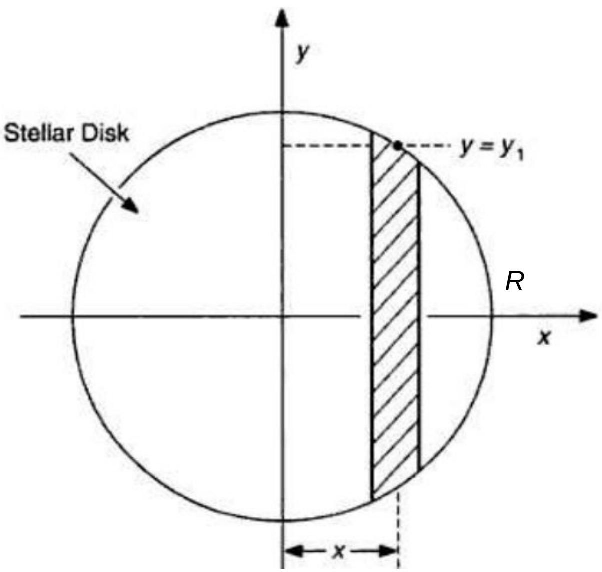

$x = R_*$ → $\Delta\lambda = \Delta\lambda_L$

$x = 0$ → $\Delta\lambda = 0$

$$F_\lambda = \frac{I_c}{R_*}\int_{-\Delta\lambda_L}^{\Delta\lambda_L}\int_{-y_1}^{y_1} H(\lambda-\Delta\lambda)\,dy\,\frac{d(\Delta\lambda)}{\Delta\lambda_L}$$

$$y_1^2 = R_*^2 - x^2$$

$$y_1^2 = R_*^2\left(1-\frac{x^2}{R_*^2}\right)$$

$$y_1 = R_*\left[1-\left(\frac{\Delta\lambda}{\Delta\lambda_L}\right)^2\right]^{1/2}$$

$I_c(\theta)$ = constant - no limb darkening

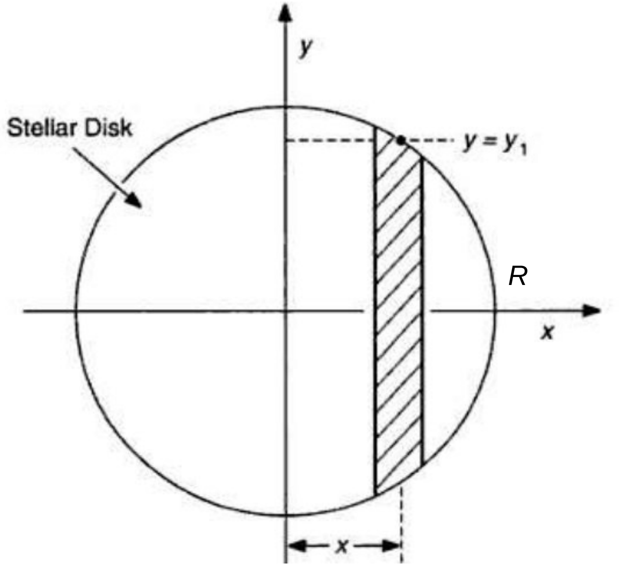

$$F_\lambda = \frac{I_c}{R_*^2} \int_{-R_*}^{R_*} \int_{-y_1}^{y_1} H(\lambda - \Delta\lambda)\, dx dy$$

$x = R_* \rightarrow \Delta\lambda = \Delta\lambda_L$

$x = 0 \rightarrow \Delta\lambda = 0$

$$F_\lambda = \frac{I_c}{R_*} \int_{-\Delta\lambda_L}^{\Delta\lambda_L} \int_{-y_1}^{y_1} H(\lambda - \Delta\lambda)\, dy \frac{d(\Delta\lambda)}{\Delta\lambda_L}$$

$$y_1^2 = R_*^2 - x^2$$

$$y_1^2 = R_*^2 \left(1 - \frac{x^2}{R_*^2}\right)$$

$$y_1 = R_* \left[1 - \left(\frac{\Delta\lambda}{\Delta\lambda_L}\right)^2\right]^{1/2}$$

$$\frac{F_\lambda}{F_{cont}} = \frac{2}{R_*} \int_{-\Delta\lambda_L}^{\Delta\lambda_L} \int_0^{y_1} H(\lambda - \Delta\lambda)\, dy \frac{d(\Delta\lambda)}{\Delta\lambda_L} \;\Big/\; \int \cos(\theta)\, d\omega_*$$

$$G(\Delta\lambda) = \frac{2}{R_* \Delta\lambda_L} \int_0^{y_1} dy \;/\; \int \cos(\theta)\, d\omega_* = \frac{2 y_1}{R_* \Delta\lambda_L \pi}$$

$$\frac{F_\lambda}{F_{cont}} = \int_{-\Delta\lambda_L}^{\Delta\lambda_L} H(\lambda - \Delta\lambda)\, G(\Delta\lambda)\, d\Delta\lambda$$

with $G(\Delta\lambda) = 0$ for $|\Delta\lambda| > \Delta\lambda_L$

$$\frac{F_\lambda}{F_{cont}} = H(\lambda) * G(\lambda)$$

$$\mathscr{F}\left[H(\lambda) * G(\lambda)\right] = \mathscr{F}\left[H(\lambda)\right] . \mathscr{F}\left[G(\lambda)\right]$$

The line profile

monochromatic line $$H(\lambda) = -\delta(\lambda - \lambda_0)$$

$$\frac{F_\lambda}{F_{cont}} = -\delta(\lambda - \lambda_0) * G(\lambda) = -G(\lambda - \lambda_0)$$

$$\frac{F_\lambda}{F_{cont}} = -\frac{2}{\Delta\lambda_L \pi}\left[1 - \left(\frac{\lambda - \lambda_0}{\Delta\lambda_L}\right)^2\right]^{1/2}$$

elliptical kernel -> elliptical profile
for narrow Voigt

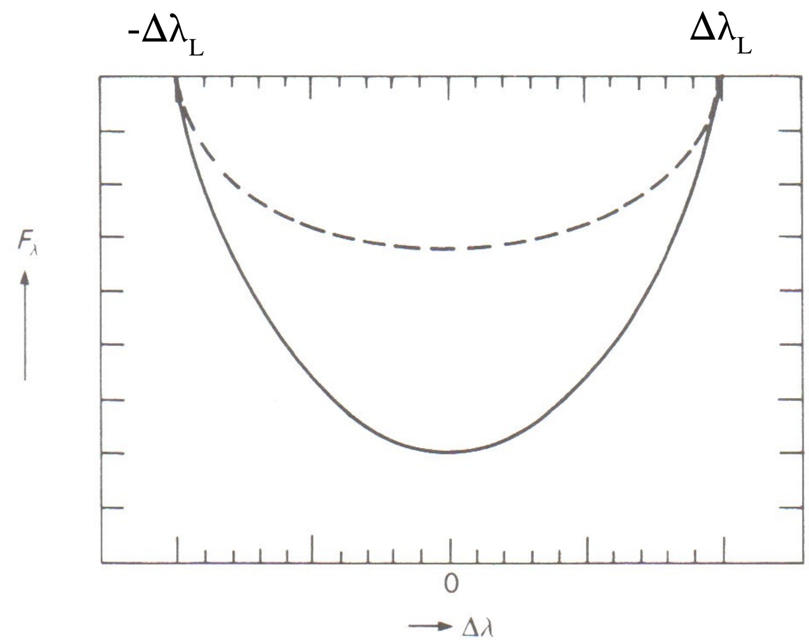

(from Bohn-Vitense 1989)

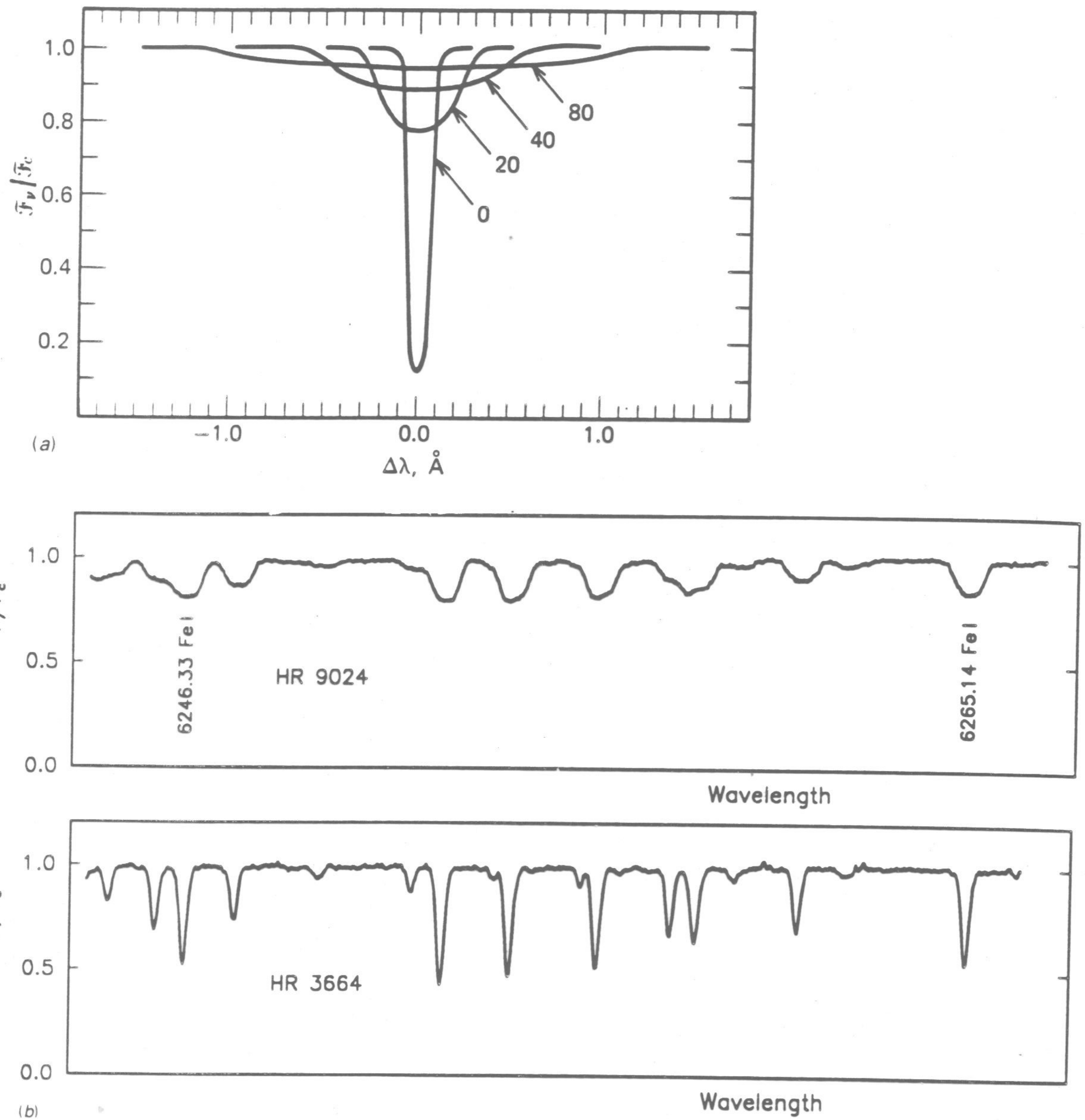

Fig. 17.7. (*a*) Computed profiles illustrate the broadening effect of rotation. The profiles are labeled with $v \sin i$, the wavelength is 4243 Å, and the line has an equivalent width of 100 mÅ. (*b*) These two early-G giants illustrate the Doppler broadening of the line profiles by rotation.

from Bohn-Vitense 1989